Colloid Polym Sci (2009) 287:725–732
DOI 10.1007/s00396-009-2020-5

ORIGINAL CONTRIBUTION

Nanocomposite particles with core-shell morphology IV: an efficient approach to the encapsulation of Cloisite 30B by poly (styrene-*co*-butyl acrylate) and preparation of its nanocomposite latex via miniemulsion polymerization

Mojgan Mirzataheri · Ali Reza Mahdavian · Mohammad Atai

Received: 1 November 2008 / Revised: 23 December 2008 / Accepted: 18 February 2009 / Published online: 4 March 2009

Abstract In this work, miniemulsion polymerization was applied for encapsulation of Cloisite 30B, an organically modified montmorillonite, inside poly (styrene-*co*-butyl acrylate) nanocomposite through an efficient and optimized procedure. The primary miniemulsions were prepared by dispersing Cloisite 30B in the monomers mixture (styrene and butyl acrylate) in the presence of sodium dodecyl sulfate and Span 80 as surfactants and hexadecane as costabilizer by using ultrasonication. The stability of both miniemulsion and the obtained latex depends on premixing procedures, time and pulsed cycle of ultrasonication, and more importantly on the applied surfactants. The synthesized products were characterized by dynamic light scattering, X-ray diffraction, transmission electron microscopy, scanning electron microscopy, induced coupled plasma, and Zeta potential measurement. Its prepared film shows an excellent transparency, which is indicative of full exfoliation of Cloisite 30B platelets by poly (styrene-*co*-butyl acrylate) latex particles through miniemulsion polymerization technique with 73% efficiency. No armored latex particle was observed.

Keywords Encapsulation · Miniemulsion polymerization · Nanocomposite · Exfoliation · Nanoclay

Introduction

By now, there have been remarkable interests and researches on the nanostructured composites, especially polymer-nanoclay composites, which present great and unique properties and applications over traditional composites [1–4]. The nanometer-size phyllosilicate platelets are prepared from natural clay minerals such as montmorillonite (MMT). They are made of two-dimensional nanoscale layers of an alumina octahedral sheet, sandwiched between two silica tetrahedron sheets that are stacked together by van der Waals and weak ionic forces and are capable of being partially or completely intercalated and exfoliated [5].

Interest in the polymer encapsulation of MMT has continued to develop because these nanocomposites offer special properties such as barrier properties [6] against liquids and gases. This is due to the large aspect ratio of MMT platelets, which is unattainable without applying nanoclay and hence has usage for barrier coatings in food packaging and agricultural and pharmaceutical industries [7, 8].

These polymer-layered-silicate nanocomposites can be synthesized by in situ intercalative polymerization such as solution [9], suspension [10], bulk [11], emulsion [12], and miniemulsion [13] techniques. Among all these techniques, only miniemulsion is capable to form nanoparticles (nanoreactors) dispersed in a continuous phase-like water for encapsulation purposes [14, 15].

There are several reports on encapsulation of inorganic particles by organic polymeric phase. Tiarks et al. encapsulated carbon black [16]. Erdem et al. achieved to encapsulate nano-TiO_2 in the polystyrene latex particles [17]. Landfester et al. have encapsulated magnetite nanoparticles in polystyrene [18]. Also, Mahdavian et al. have prepared nanocomposite latex particles based on magnetite, silica, and alumina through emulsion or miniemulsion polymerization [19–21].

Miniemulsion polymerization, a branch of conventional emulsion polymerization comprising a small amount of a

M. Mirzataheri · A. R. Mahdavian (✉) · M. Atai
Polymer Science Department, Iran Polymer & Petrochemical Institute, P.O. Box 14965/115, Tehran, Iran
e-mail: a.mahdavian@ippi.ac.ir

material called costabilizer (water-insoluble, monomer soluble), provides the conditions needed for the encapsulation of a layered clay. This is performed by reducing the diffusional degradation (Ostwald ripening) of a monomer/water emulsion as well as diminishing the monomer droplet size to within a range of 50–500 nm via applying high shear [5, 22], and the monomer droplets become the primary loci for particle nucleation. Deng et al. synthesized encapsulated laponite–polystyrene composites [5]. They have also studied the encapsulation of nanosaponite in polystyrene [1]. All of these researchers have applied miniemulsion polymerization techniques for encapsulation purposes.

It is obvious that clay and nanoclay exfoliation lies in the synergistic effect of chemical and mechanical interactions. Under strong mechanical force of ultrasonication, the polymer particles tend to stick to the organoclay surface, forming clay–polymer microaggregates that could be stabilized by adding surfactant or dispersing agents such as Span 80. By further applying mechanical force to the system, although it is in a water dispersion form, the polymer molecules could be enforced to diffuse into the basal spacing of the nanoclay and thus resulting in an exfoliated nanocomposite suspension [23]. It is well known that MMT has a platy structure with a broad aspect ratio and size distribution, resulting in more difficulties for encapsulation in the monomer droplets and polymer latex particles even through miniemulsion polymerization [1, 24].

To date and to the best of our knowledge, no report exists that describe the encapsulation and, thereafter, exfoliation of Cloisite 30B (organically modified MMT [25]) inside copolymer particles except what has been recently published about MMT [26]. Here, the reports on various kinds of clay such as laponite, saponite, illite, and magadiite have not been considered since their structure, shape, and morphology are quite different from Cloisite 30B (as a smectite clays with plate-shaped and nanometer-sized in thickness).

In this study, miniemulsion polymerization approach was used to synthesize encapsulated poly (styrene-*co*-butyl acrylate) nanocomposite latex particles, including Cloisite 30B. The affecting factors were also examined in detail by using of dynamic light scattering (DLS), X-ray diffraction (XRD), scanning electron microscopy (SEM), transmission electron microscopy (TEM), inductively coupled plasma (ICP), and Zeta potential analysis. It was proved that sodium dodecyl sulfate (SDS) molecules not only favored clay dispersion in the oil droplets but also aided the entry of monomers into the clay intergalleries during polymerization when it was used in conjunction with the nonionic surfactant such as Span 80. Here, Cloisite 30B was significantly encapsulated within the polymeric shell and formed a stable latex particle as the polymerization initiated and progressed through intergalleries of the clay. This expanded and exfoliated the MMT platelet arrays to form a fully exfoliated structure. Quantitatively, encapsulation efficiency was also determined.

Experimental

Materials

Commercially available organoclay Cloisite® 30B, a natural montmorillonite modified with an organic modifier named methyl tallow bis-2-hydroxyethyl quaternary ammonium chloride (MT2EtOHCl), was supplied from Southern Clay Products [25] (Gonzales, USA), with d_{001}=1.74 nm (measured in our laboratory) that was further ground by mortar and pestle. SDS from Aldrich, hexadecane (99%) and styrene (99%) from Merck Chemical, and also butyl acrylate (99%) from Fluka Chemical were purchased and used as received. Styrene was purified by two times washing with 5% aqueous NaOH solution (*W/V*) and subsequently with plenty of distilled water until pH of the separated aqueous phase was reached to 7.0 and stored on dried $CaCl_2$ at 0 °C prior to use. Span 20, 40, 60, and 80 (sorbitan derivatives with various M_n) were purchased from Merck Chemical and used as received. 2, 2′-Azo isobutyronitrile (AIBN) was a product of Fluka and used as initiator. It was kept refrigerated prior to use.

Na_2CO_3 from Iranian Arastoo used as buffer and all other reagents were analytical grade and were used as received.

Characterization

FT-IR spectra were recorded on EQUINOX55, Bruker (Germany) from the prepared KBr pellet samples. X-ray diffraction patterns were recorded on a Siemens D5000 (Germany) using Cu Kα ray (λ=1.54056 Å) as the radiation source, with a step size of 0.02° and a scan step time of 1 s. The d_{001} basal spacing of the samples was calculated using the Bragg equation ($d=\lambda/2 \sin \theta$, where λ is the incident wavelength (1.54056 Å), and θ is the diffraction angle [27].)

The particle size and its polydispersity were measured by a dynamic light scattering on a SEM 633 from SEMATech (France) at fixed angle of light at 90°, 25 °C, and under laser beam (λ=633 nm). The samples were diluted with an aqueous solution containing SDS and Span 80 in the same concentration as its mother liquor to reduce the dilution effect on droplet size [5]. TEM observations on the morphology of latex particles were conducted on a CEM-902A, Zeiss (Germany) at an accelerating voltage of 80 kV. The samples were prepared by casting a drop of 40 times diluted latex solution onto a 200-mesh covered Formvar/carbon coated copper grid at room temperature and dried at 60 °C overnight.

SEM analysis was carried out on a tungsten-heated cathode, TESCAN model VEGAII XMU from Czech Republic. The samples were gold-coated in high vacuum mode (30 kV, 20 μA) with thickness less than 3 nm in less

Table 1 Typical recipe for the miniemulsion polymerization of poly (styrene-*co*-butyl acrylate)–Cloisite 30B nanocomposite latex particles

Mixture	Component	Added amount (g)	Wt.% relative to the total monomers
Phase I	Styrene	12.73	100.0
	Butyl acrylate	6.27	
	Cloisite 30B	1.00	5.3
	Hexadecane	1.14	6.0
	Span 80	0.10	0.5
Phase II	Water	78.00	410.5
	Span80	0.20	1.0

than 3 min and working vacuum pressure of 9.9×10^{-3} Pa inside the chamber in order to dry the sample before gold coating. ICP measurements were carried out by VARIAN model VISTA-PRO (Australia) equipped with a detector of CCD simultaneous ICP-OE5 and radial torch. The media for ICP analysis was toluene. The dispersions were prepared in a Julabo Labortechnik GMBH D-733 Seelbach (Germany) ultrasound bath with frequency of 35 KHz. Direct ultrasonication (probe immersed in the samples) was performed by 20 kHz±500 Hz ultrasonic generator, SONOPULS ultrasonic homogenizer, Model HEGM 2200 from BANDELIN Electronic GmbH & Co. KG (Germany), and the used probe was a titanium microtip MS-73 with a 3 mm diameter from the above company used at pulsed mode and a power of 80%. Films of the obtained polymeric latexes were prepared at 250 °C under 100 bar pressure with thickness of 150 μm by compression molding machine from ALEEY (Iran). Zeta potential distribution was measured by Malvern Zetasizer Nano ZS (England) on equally diluted samples with an aqueous solution containing SDS and Span 80 with the same concentration as its mother liquor in order to reduce the dilution effect on particle size and zeta potential of particles surface.

Miniemulsion polymerization of styrene/butyl acrylate in the presence of Cloisite 30B

According to the previous reports [27–29], purification and intercalation can significantly reduce the clay aspect ratio. So, nanoclay was grinded by mortar and pestle finely. As indicated in Table 1, phase I composed of Cloisite 30B, styrene, butyl acrylate, hexadecane, and Span 80 was under magnetic stirring (300 rpm) for 1 h at room temperature and kept cool in refrigerator for 15 min. Then, it was placed in an ultrasound bath for 30 min. Meanwhile, aqueous phase II was prepared of distilled water and Span 80 under simple stirring at room temperature for 15 min and then kept cool in the refrigerator for 15 min. Phase I and phase II were mixed under vigorous magnetic stirring (700 rpm) for 15 min. Then, SDS (0.2 g) was added to the above dispersion, and further homogenization and ultrasonication was conducted with the sonicator probe for 4 min. The obtained miniemulsion with solids content of 20% was used for subsequent polymerization.

To the as-prepared miniemulsion in a four-necked 250-mm glass reactor equipped with condenser, AIBN (0.28 g) was added and subsequently degassed by N_2 at room temperature for 30 min. Then, it was placed in a water bath at 60 °C, and the temperature was kept constant during polymerization reaction.

The polymerization was conducted at this temperature for 6.5 h under continuous mechanical stirring (300 rpm) in the presence of sodium bicarbonate (0.2 g) as buffer. The reaction was terminated by adding one drop of 1% (*W/V*) hydroquinone solution in methanol into the latex sample. Concentrated milky miniemulsion latex was obtained with final conversion of 95.4% and 1 wt.% coagulum content.

Table 2 Calculated *d*-spacing of the samples measured by XRD in the presence of span series

Samples	Surfactant	d_{001} (nm)
S1-20	Span 20	1.45
S2-40	Span 40	1.42
S3-60	Span 60	1.43
S4-80	Span 80	1.47

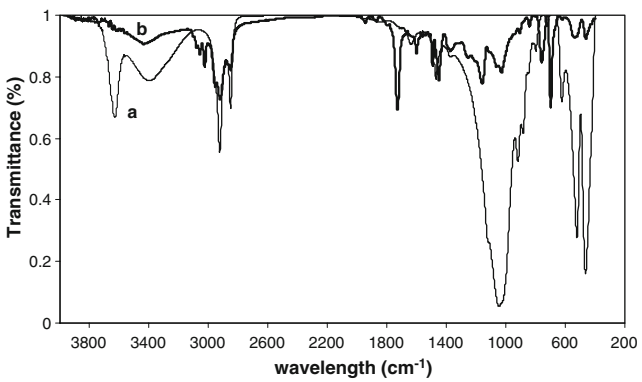

Fig. 1 The FT-IR spectra: *a* Cloisite 30B, *b* as prepared nanocomposite, including 5.3 wt.% of encapsulated Cloisite 30B

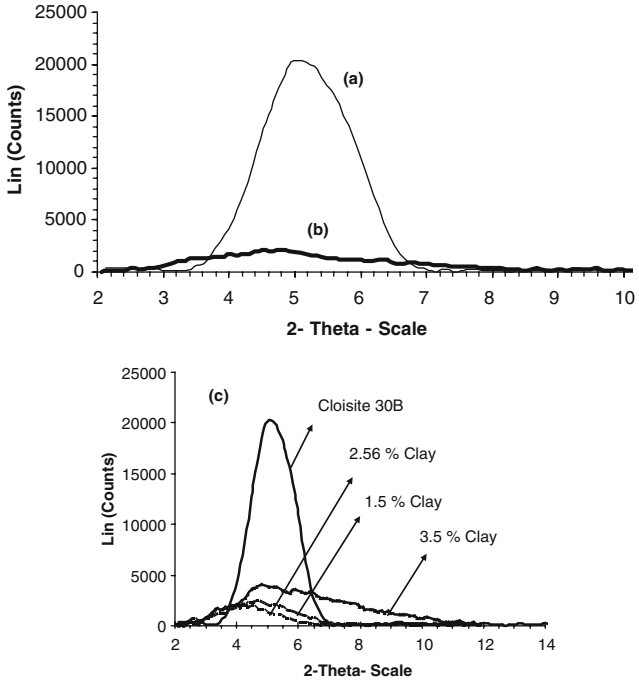

Fig. 2 XRD spectra: (*a*) pristine Cloisite 30B, (*b*) poly (styrene-*co*-butyl acrylate)–Cloisite 30B nanocomposite, including 5.3 wt.% of exfoliated Cloisite 30B, (*c*) poly (styrene-*co*-butyl acrylate)–Cloisite 30B nanocomposite, including 1.5, 2.56, and 3.5 wt.% Cloisite 30B

Results and discussion

The effect of surfactant

Cloisite 30B is a modified montmorillonite with methyl tallow bis-2-hydroxyethyl quaternary ammonium [MT2EtOH] (d_{001}=1.74 nm). In order to have its good dispersion in the organic phase [30], a series of experiments (S1-20, S2-40, S3-60, and S4-80) were designed using Span surfactants (20, 40, 60, and 80). In all experiments, Cloisite 30B (1 g) was dispersed in 100 g distilled water under vigorous magnetic stirring for 1 week at 50°C. Then, Span (0.3 g) and SDS (0.2 g) were added to this dispersion under magnetic stirring for about 2 days at 50°C. Finally, the mixture was dried at 80°C for 24 h, and then it was ground into the powder and used for XRD analysis (Table 2). The results showed that the *d*-spacing decreased to 1.4 nm. It seems that SDS molecules have the ability to extract the clay's modifier (MT2EtOH, a quaternary ammonium salt) in the presence of water and Span surfactant. This is due to the occurrence of cation exchange for SDS, which results in the withdrawal of modifier from interlayers for the modified clay. On the other hand, Span molecules are not able to penetrate into the interlayer space of Cloisite 30B according to their long-carbon-chain structure. Therefore, a decrease in the interlayer spacing was observed, and in order to keep the clay modifier in its primary position, SDS was added just at the beginning of miniemulsion preparation.

The final poly (styrene-*co*-butyl acrylate)–Cloisite 30B nanocomposite particles prepared via miniemulsion polymerization were characterized by FT-IR analysis primarily. Figure 1 shows the FT-IR spectra of Cloisite 30B and final poly (styrene-*co*-butyl acrylate)–Cloisite 30B nanocomposite, respectively.

For preparing nanocomposite spectra (Fig. 1 b), the latex was coagulated with methanol. Then, the coagulum was separated from the aqueous phase and washed with distilled water in order to separate the non-encapsulated clay or adsorbed ones. The coagulated polymer was dried at 60°C in an oven overnight for taking FT-IR spectrum. In Fig. 1 a, the peak at 3,438 cm^{-1} corresponds to OH stretching of silicate layers. The sharp peak centered at 1,028 cm^{-1} is related to the Si–O stretching vibration of silicate layer too. The peaks at 531 and 461 cm^{-1} are due to the stretching of Al–O and bending of Si–O, respectively [31]. Figure 1 b clearly demonstrates the existence of Cloisite 30B major absorbance peaks in poly (styrene-*co*-butyl acrylate) spectrum [32], which proves the existence of clay inside the dried latex particles and indicative of encapsulation of Cloisite 30B inside the final nanocomposite particles.

XRD analysis of Cloisite 30B and its nanocomposite

The exfoliation of some polymer/organically modified clay composites was investigated using XRD analysis [30]. The final latex obtained from miniemulsion polymerization was powdered off in the liquid nitrogen, dried, and used for XRD measurement (Fig. 2). Cloisite 30B has an interlayer spacing of 1.74 nm at 2θ ca. 5.08° calculated from Bragg equation (d_{001} is the interplanar distance of (001) reflection plane). The XRD patterns of pristine Cloisite 30B and its nanocomposite have been shown in Fig. 2 a and b, which clearly depict the disappearance of clay sharp peak (appears at 5.08°) in the obtained nanocomposite. This implies a full

Table 3 Zeta potential results for polymeric latexes

Sample	Zeta potential (mv)	Mean (mv)	Area (%)	Width (mv)
Poly (styrene-*co*-butyl acrylate) without Cloisite 30B	−60.2	−60.0	100.0	6.96
Poly (styrene-*co*-butyl acrylate) with 5.3 wt.% Cloisite 30B	−40.1	−40.1	100.0	7.83

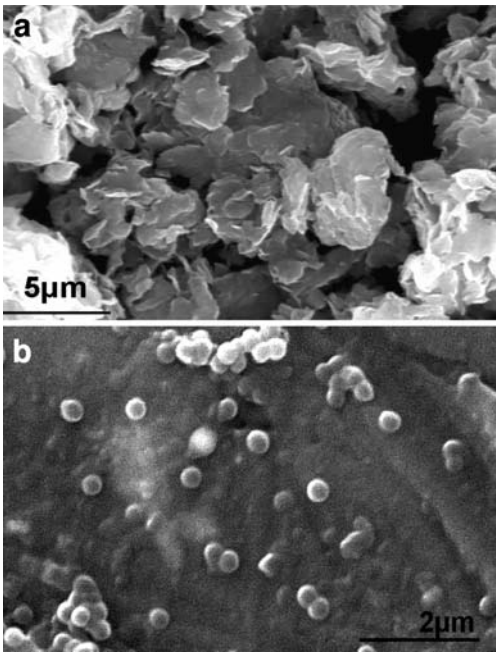

Fig. 3 SEM micrographs of **a** pristine Cloisite 30B before grinding and high ultrasonic shear, **b** poly (styrene-*co*-butyl acrylate)–Cloisite 30B nanocomposite particles containing 5.3 wt.% of encapsulated Cloisite 30B

exfoliation of Cloisite 30B in the final nanocomposite. It is suggested that SDS, with high anionic charge density, has the capability to enter into the basal surfaces of Cloisite 30B by formation of ionic networks with the modifier segment. It will increase the hydrophobicity of intergalleries due to the presence of long alkyl chain in SDS. This is the key factor for intercalation of clay [15], which helps in exfoliation process through insertion of monomer molecules and subsequent polymerization. In another point of view, SDS can strongly adsorb onto the OH groups on the edges of clay platelets, which influence not only the colloidal stability but also exfoliation of the platelets by decreasing clay hydrophilicity. The applied high shear through ultrasonication also plays an important role in progress of exfoliation process. Thus, SDS molecules could help to enter comonomers to make the gap between clay layers wider. Also, polar carboxyl groups of butyl acrylate are able to interact with the polar groups in the intergalleries.

This will aid in the further continuous entry of bulky styrene monomer into the intergalleries and enforce the clays' layers for more exfoliation. Thereafter, we synthesized poly (styrene-*co*-butyl acrylate)–Cloisite 30B nanocomposite particles containing 1.5, 2.56, and 3.5 wt.% Cloisite 30B with the same recipe for 5.3 wt.%. Their XRD patterns (Fig. 2 c) strongly confirmed the disappearance of pristine Cloisite 30B sharp peak (at 5.08°), which implies a full exfoliation of pristine Cloisite 30B in their final nanocomposites.

Moreover, the recorded zeta potential distribution for poly (styrene-*co*-butyl acrylate) without clay and poly (styrene-*co*-butyl acrylate) with 5.3 wt.% Cloisite 30B (Table 3) proved our theory about the role of the SDS molecules in exfoliation of the Cloisite 30B platelets more precisely. SDS could enter into the intergalleries of clay since a remarkable decrease in surface potential of the prepared nanocomposite latex particles was observed relative to the primary poly (styrene-*co*-butyl acrylate) without any clay. This indicates a reduction in the appearance of surfactant molecules on the surface of particles and thereof their logical entrance between clay platelets. Due to the relatively negative charge of clay platelets, it is deducible that no armored latex particle is formed since in this case the observed zeta potential of the latex would be increased.

In this way, intercalation and exfoliation of Cloisite 30B and its final encapsulation could be achieved due to the applied miniemulsion polymerization conditions.

Studies on size and morphology of the particles

According to Fig. 3, the synthesized final latex nanocomposite particles via miniemulsion polymerization, using AIBN as initiator and SDS as ionic surfactant, are mainly composed of spherical particles in a range of 100–300 nm with average diameter size of 230 nm. They seem to have smooth surfaces without any attached or adsorbed clay on the particles' surface.

Furthermore, as shown in Table 4, average particle size of the final product in the presence of Cloisite 30B from DLS analysis was bigger with a broader particle size distribution in comparison with those without any organo-

Table 4 The particle size and its distribution measured by DLS analysis

Sample	Average diameter (nm)	Standard deviation	Particle size distribution
Poly (styrene-*co*-butyl acrylate) without Cloisite 30B	138	0.31	93.9% below 238 nm 6.1% between 238 and 500 nm
Poly (styrene-*co*-butyl acrylate) with 5.3 wt.% Cloisite 30B	250	0.24	92.1% below 441 nm 7.9% between 441 and 700 nm

Table 5 Effect of sonication pulsed cycle on particle sizes obtained at various intervals for the sample containing 5.3 wt.% Cloisite 30B

Various intervals of experiment	Particle size (nm)	
	1[a]	9[b]
Before ultrasonication with probe	260	260
After ultrasonication with probe	230	464
At the end of polymerization	250	1,541

[a] Ultrasonication is active for 0.1 s per each second

[b] Ultrasonication is active for 0.9 s per each second

clay. The observed increase after addition of clay could be a further evidence of an effective encapsulation through polymerization reaction beside the other analysis techniques such as SEM, TEM, and ICP, which will be discussed in the next.

In another observation, the effect of ultrasonication pulsed cycle [(cycle)×10%] per second on dispersion stability was studied (Table 5). At the pulsed cycle of 1, the coagulation content of polymerization reaction was negligible that indicates a reasonable stability of the final latex. Stability of the final latex decreases rapidly by increasing pulsed cycle from 1 to 9. This is according to the coalescing of minidroplets during the process that leads to a remarkable increase in particle size.

The concentration range and effective time of adding surfactants were also screened and found that they had a positive effect on the clay dispersability in the latex particles (Table 6).

The stability of obtained nanocomposite final latex, including 5.3 wt.% of Cloisite 30B, has been shown below (Fig. 4). It was observed that the latexes were completely stable during about 100 days.

For further investigation of morphology of the obtained nanocomposite particles and verifying exfoliation of Cloisite

Table 6 Stability of Cloisite 30B in poly (styrene-*co*-butyl acrylate)–Cloisite 30B Nanocomposite

Sample	Composition	Note
ST-1	Base recipe (Table 1)	Formation of precipitates up to 3 h after the end of polymerization reaction
ST-2	0.1 g more Span 80 was added in phase II of ST-1 recipe	Formation of lower amounts of precipitates up to 6 h after the end of polymerization reaction
ST-3	0.1 g extra SDS was added after progress of polymerization of ST-2 reaction for 2 hrs	Homogenous and stable latex for more than 15 h after the end of polymerization reaction

Fig. 4 Colloidal stability of a nanocomposite latex, including 5.3 wt. % Cloisite 30B at different intervals of 30 days (ST-5), 60 days (ST-6), 90 days (ST-7), and 100 days (ST-8)

30B, TEM micrographs were taken by dropping diluted latex on TEM copper grids. One of the samples was dried at room temperature (Fig. 5a), and the other one was heated up to 60 °C (after drying at room temperature) to form a thin film on the grid (Fig. 5b). These micrographs are indicative of encapsulation (dark domains inside polymer particles) and exfoliation (stretched and separated lines) of Cloisite 30B platelets, which were uniformly dispersed inside the final synthesized latex particles via miniemulsion polymerization. No clay armored latex particle was observed [33].

For ICP measurements, firstly, we checked and observed that addition of methanol into the dispersion of 5.3 wt.% clay in water had no effect on the homogeneity of the whole system. Therefore, a certain amount of latex was coagulated with methanol, and then it was washed with distilled water and dried at 60 °C (for 24 h.). Afterward, the coagulum was dissolved in toluene and filtered off in order to remove non-encapsulated and non-exfoliated Cloisite 30B as it is not dispersible in toluene. Then, the solution was analyzed by ICP for measuring the percentage of silicon (Si%) with respect to the encapsulated Cloisite 30B inside polymer particles. ICP analysis showed 10.9 ppm Si averagely, which provides complementary evidence that not only the nanoclay (Si is its major element in the structure) was encapsulated but also its encapsulation efficiency was 73%. Theoretical value for 100% encapsulation of clay inside the polymer latex particles should be 15.2 ppm based on its added amount in the base formulation.

Finally, both films of pure poly (styrene-*co*-butyl acrylate) and poly (styrene-*co*-butyl acrylate)–Cloisite 30B nanocomposite, including 5.3 wt.% Cloisite 30B, were prepared with thickness of 150 μm at 250° C under pressure of 100 bar by compression molding. As was shown in Fig. 6, these films had excellent transparency and clarity, which is another reason for full exfoliation of clay inside the polymeric phase, and there is no pristine or aggregate of the clay in the corresponding film.

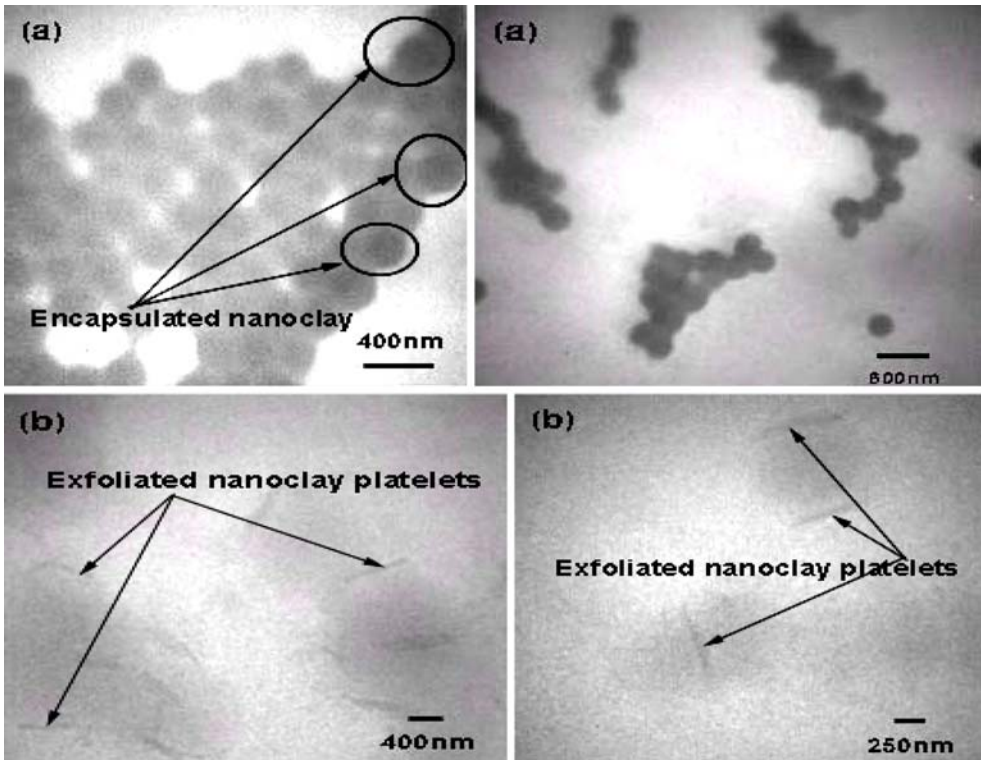

Fig. 5 TEM micrographs of poly(styrene-*co*-butyl acrylate)–Cloisite 30B nanocomposite, including 5.3 wt.% of encapsulated Cloisite 30B: **a** dried at room temperature, **b** after heating up to 60 °C

All these results confirmed that Cloisite 30B was encapsulated efficiently and fully exfoliated inside the polymer latex particles.

Conclusion

In this work, fully exfoliated encapsulated Cloisite 30B (modified montmorillonite) was prepared by using nonionic-ionic surfactant mixture, which were very efficient in stabilizing the nanocomposite latex particles. In conclusion, it has been demonstrated that the encapsulation of clay platelets in the presence of SDS surfactant was successful since some parts of it can interact with cationic modifier of clay (METtOH) and keep SDS molecules between the intergalleries of clay. This makes these spaces more organophilic and helps the comonomers entry for exfoliation and results in further expansion of the clay galleries to accommodate the polymer chains.

Fig. 6 Films of pure poly (styrene-*co*-butyl acrylate) (*ST-I*) and poly (styrene-*co*-butyl acrylate)–Cloisite 30B nanocomposite, including 5.3 wt.% Cloisite 30B (*ST-II*)

On the other hand, SDS can strongly adsorb onto the OH groups on the edges of clay platelets, which influence not only the colloidal stability but also exfoliation of the platelets by decreasing clay hydrophilicity. Here, poly (styrene-*co*-butyl acrylate)–Cloisite 30B nanocomposite stable latex was prepared via miniemulsion polymerization. The procedure and addition sequence were the key factors of 73% encapsulation efficiency and full exfoliation of Cloisite 30B inside the stable latex particles. According to DLS analysis, SEM and TEM images, mono-size spherical particles within a size from 100 to 300 nm, were prepared. Furthermore, the morphology of final latex particles proved that Cloisite 30B was encapsulated inside the polymer latex particles that had smooth surfaces without any attached clay platelets on the polymer particles surfaces as id usually observed in the clay-armored latex particles. It is noteworthy that according to the TEM images and prepared transparent films of the obtained nanocomposite, exfoliated Cloisite 30B platelets were uniformly dispersed in the polymeric matrix.

Acknowledgments Valuable comments and suggestions from Prof. A. M. van Herk (Eindhoven University of Technology) after reviewing the manuscript are greatly acknowledged. We wish to express our gratitude to Iran Polymer & Petrochemical Institute (IPPI) for financial support of this work (grant no. 24751102) and also Mr. Hashemi for helpful assistance from Faculty of Science, University of Tehran in taking TEM micrographs.

References

1. Tong Z, Deng Y (2007) Polymer 48(15):4337–4343
2. Utracki LA, Sepehr M, Boccaleri E (2007) Polym Adv Technol 8 (1):1–37
3. Ray SS, Okamoto M (2003) Prog Polym Sci 28(11):1539–1641
4. Diaconu G, Asua JM, Paulis M, Leiza JR (2007) Macromol Symp 259:305–317
5. Sun Q, Deng Y, Wang ZL (2004) Macromol Mater Eng 289 (3):288–295
6. Giannellis EP (1996) Adv Mater 8(1):29–32
7. Pinnavaia TJ, Beall GW (eds) (2001) Polymer-clay nanocomposites. Wiley, New York
8. Gopakumar TG, Page DJYS (2005) J Appl Polym Sci 96 (5):1557–1563
9. Shah D, Fytas G, Vlassopoulos D, Di J, Sogah D, Giannelis EP (2005) Langmuir 21(1):19–25
10. Luo J-J, Daniel IM (2003) Composites Sci Tech 63(11):1607–1616
11. Aguilar-Solis C, Xu Y, Brittain W (2002) J Polym Preprints 43 (2):1019–1023
12. Negrete-Herrera N, Persoz S, Putaux J-L, David L, Bourgeat-Lami E (2006) J Nanosci Nanotech 6:421–431
13. Tong Z, Deng Y (2006) Ind Eng Chem Res 45(8):2641–2645
14. Landfester K (2003) Colloidal chemistry II. In: Markus A (ed) Topics in current chemistry, vol 227. Springer, Berlin, pp 75–123
15. Moraes RP, Santos AM, Oliveira PC, Souza FCT, Amaral Md, Valera TS, Demarquette NR (2006) Macromol Symp 245–246:106–115
16. Tiarks F, Landfester K, Antonietti M (2001) Macromol Chem Phys 202(1):51–60
17. Erdem B, Sudol ED, Dimonie VL, El-Aasser MS (2000) J Poly Sci Part A: Polym Chem 38(24):4441–4450
18. Ramirez LP, Landfester K (2003) Macromol Chem Phys 204 (1):22–31
19. Mahdavian AR, Ashjari M, Bayat Makoo A (2007) Eur Polym J 43:336–344
20. Mahdavian AR, Ashjari M, Salehi-Mobarakeh H (2008) J Appl Polym Sci 110:1242–1249
21. Mahdavian AR, Sehri Y, Salehi-Mobarakeh H (2008) Eur Polym J 44:2482–2488
22. Reimer JL, Schork F (1997) J Ind Eng Chem Res 36:1085–1088
23. Sun Q, Schork FJ, Deng Y (2007) Composites Sci Tech 67 (9):1823–1829
24. Voorn DJ (2006) Encapsulation of platelets by physical and chemical approaches, PhD Thesis. Technical University of Eindhoven, Eindhoven
25. Southern Clay Products Inc., Subsidiary of Rockwood Additives, www.scprod.com
26. Bouanani F, Bendedouch D, Hemery P, Bounaceur B (2008) Colloids & Surfaces A: Physicochem Eng Aspects 317:751–755
27. Utracki LA (2004) Clay-containing polymeric nanocomposites. Rapra, Shropshire
28. Sun QH, Xu KT, Peng H, Zheng RH, Haussler M, Tang BZ (2003) Macromolecules 36(7):2309–2320
29. Ferreiro V, Schmidt G, Han CC, Karim A (2000) Polymer nanocomposites, ACS Symposium Series 804. Chapter 14. American Chemical Society, Washington DC
30. Jeon HS, Rameshwaram JK, Kim G (2004) J Polym Sci Part B: Polym Phys 42(6):1000–1009
31. Xu M, Choi YS, Kim YK, Wang KH, Chung IJ (2003) Polymer 44(20):6387–6395
32. Hummel DO, Scholl F (1990) In Atlas of polymer and plastics analysis, 2nd edn, vol 2, Part A/II. Car Hanser Verlag, Munich
33. Cauvin S, Colver PJ, Bon SAF (2005) Macromolecules 38 (19):7887–7889